Applied Thermal Engineering 84 (2015) 286–291

Contents lists available at ScienceDirect

Applied Thermal Engineering

journal homepage: www.elsevier.com/locate/apthermeng

Research paper

Theoretical estimation of solidification length of continuously cast metals

Pavan Kumar Penumakala [a], Ashok Kumar Nallathambi [a,*], Eckehard Specht [a], Ulrich Urlau [b], Paulina Unifantowicz [b]

[a] Otto von Guericke University Magdeburg, Germany
[b] SWISS STEEL, Switzerland

HIGHLIGHTS

- Guidelines are presented for designing a new continuous casting process.
- Model is developed with a constant surface temperature assumption.
- 2-D conduction equation is solved including the solidification effect.
- Solidification length increases with mass flow and surface temperature.
- Solidification length decreases with increase in width to thickness ratio.

ARTICLE INFO

Article history:
Received 25 November 2014
Accepted 26 March 2015
Available online 4 April 2015

Keywords:
Solidification
Phase change
Heat transfer
Continuous casting
Secondary cooling
Stefan number

ABSTRACT

A semi-analytical model is presented to find the solidification length of continuously cast metals. An existing theoretical solution for solidification in an infinite slab, which is maintained at constant surface temperature is extended to a finite slab. For the case of a finite slab, the governing 2-D heat conduction equation is solved in the non dimensional form using a constant surface temperature as a boundary condition. The solution also delivers the guidelines for the kind of cooling profile which has to be applied in reality. It is found that the total solidification length (metallurgical length) in a continuous casting process is proportional to the mass flow rate and specific heat capacity and inversely proportional to the conductivity and width to thickness ratio of the slab. The novelty of this study is that it provides design guidelines for the process engineers to find the solidification length beforehand for a given cast alloy and ingot geometry.

1. Introduction

Continuous casting is a well established technique for casting metals such as steel, copper, aluminum *etc*. During the continuous casting, the total heat from the molten metal is extracted in a controlled manner in primary mold cooling and in the secondary water cooling. It is necessary to predict the heat transfer in these zones to find the location where the complete solidification occurs. Stefan was the first person who studied the freezing of ice and introduced the concept of moving interface [1]. A lot of research has been published in the literature to analyze the mold and secondary cooling heat transfer in a continuous casting. The quantitative analysis of the mold heat transfer was pioneered by J. K. Brimacombe [2,3]. Grill et al. presented a mathematical model to analyze the heat transfer and gap formation in the mold and investigated the conditions which can lead to breakouts [4]. Alizadeh et al. presented an analytical expression for the heat flux in the mold that includes practically controllable parameters such as mold height, cooling water flow rate and the cooling water temperature rise [5]. Straffelini et al. used the water flow dependent relation in the secondary cooling zone to calculate the local heat transfer coefficient [6]. Meng et al. takes into account the influence of rollers on heat transfer [7]. Ha et al. presented a 1-D numerical model to find the temperature and solidification length of slab casting [8]. Many 2-D slice models are presented to simulate the temperature evolution and the final solidification point of continuous casting [9].

* Corresponding author. Otto von Guericke University Magdeburg, Universitätsplatz 2, 39106 Magdeburg, Germany. Tel.: +49 3916752737; fax: +49 3916752762.
E-mail address: ashok.nallathambi@ovgu.de (A.K. Nallathambi).

http://dx.doi.org/10.1016/j.applthermaleng.2015.03.060
1359-4311/

Nomenclature

T_f	liquidus temperature (°C)
T_s	solidus temperature (°C)
T_w	surface temperature (°C)
λ	thermal conductivity (W/mK)
c	specific heat (J/kgK)
ρ	density (kg/m^3)
Δh	latent heat (J/kg)
a	thermal diffusivity (m^2/s)
V_c	casting speed (m/min)
$\theta = \frac{T-T_w}{T_f-T_w}$	dimensionless temperature
$X = \frac{x}{s/2}$	dimensionless space coordinate
$\Delta = \frac{\delta}{s/2}$	dimensionless solidification thickness
$Fo = \frac{at}{(s/2)^2}$	Fourier number
$Ste = \frac{c(T_f-T_w)}{\Delta h}$	Stefan number
B	width of the ingot
s	thickness of the ingot
δ	solidified layer thickness
$\dot{M}$	mass flow rate

Wang et al. investigated the effect of casting speed, slab size and superheat on temperature and the final solidification length using a 2-D slice approach [10].

The twin-belt caster received major attention for its excellent performance in the continuous casting of nonferrous metals [11]. Farouk et al. investigated the effect of process parameters on the heat transfer and solidification in a twin-belt caster [12]. Gerber et al. demonstrated that belt heat transfer and casting speed are most influential on solidification [13].

Even though many studies are presented in analyzing the existing continuous casting process, theoretical guidelines to design the plant based on the final solidification length are not yet well established. Therefore, a generalized theoretical model which incorporates all kind of metals is developed and the key design parameters are identified. The cooling strategies in different zones are normally obtained from the costly industrial trails. From the solution of the model developed, it is easier to design the secondary cooling spray arrangements which eliminates the heuristic approach.

2. Methodology

2.1. Assumptions

Fig. 1 shows the typical temperature profiles during the continuous casting process of steel. It is observed that the surface temperature drops to a certain value at the mold exit and fluctuates up and down over the range of temperature in the secondary cooling zone. The local oscillations in the temperature are due to the cooling by sprays with varying impingement density. The arrangement of nozzles causes the strand to heat and cool intermittently. Beyond the secondary cooling zone, the surface temperature increases suddenly and then slowly decreases due to the radiation mode of heat transfer. For the purpose of developing a theoretical solution, the surface temperature is approximated as constant from the beginning till the end of solidification. The temperature drop in the mold region is neglected because the mold length is typically less than 1 m, which is only 5–10 % of the total solidification length. It is observed that the core temperature does not change till the complete solidification. The effect of constant surafce temperature will not be felt at the core till the solidification front reaches.

Even though the constant surface temperature assumption is not correct, it is a worthful, valid and convincing one for the production personnel. The work in this manuscript is undertaken with the objective of providing guidelines for designing a new casting process. When there is no information about the convective heat transfer coefficient, it is better to assume infinite heat transfer coefficient i.e. constant surface temperature. After finding the required heat flux from the solution, it is better to achieve the finite heat transfer coefficient using the sprays. Due to this reason the work is carried out with constant surface temperature assumption. Due to this assumption, it is possible to set the benchmark model parameters for the design of new casting process for metals. In the later stage, one can search for sophisticated commercial packages for simulating the exact situation. The detailed numerical simulation of the designed casting process is only useful for optimizing the process, but not for providing the initial design guidelines.

2.2. Semi infinite slab

Consider a half-domain of length (s/2) which contains fully molten metal at the liquidus temperature T_f as shown in Fig. 1. If the surface is maintained at a constant temperature T_w, which is well below T_f, solidification starts from the surface. The solid phase grows with time and the solidification front moves along the positive x-direction. The domain is considered as a semi infinite body for transient heat conduction and the heat transfer is purely one dimensional. Fig. 1 shows the typical temperature profiles at different times t_1, t_2 and t_f. The heat conduction in the solidified layer is governed by the Fourier differential equation of the form [14].

$$\rho c \frac{\partial T}{\partial t} = \lambda \frac{\partial^2 T}{\partial x^2}. \tag{1}$$

The initial and boundary conditions are

$$T(x, t=0) = T_f, \quad T(x=\delta, t) = T_f, \quad T(x=0, t) = T_w. \tag{2}$$

The solid growth rate is controlled by the energy balance at the solidification front, which can be written as

$$\lambda \cdot \frac{\partial T}{\partial x}(x=\delta) = \Delta h \cdot \rho \cdot \frac{d\delta}{dt}. \tag{3}$$

The above system of equations can be written in the dimensionless form as,

$$\frac{\partial \theta}{\partial Fo} = \frac{\partial^2 \theta}{\partial X^2}. \tag{4}$$

$$\theta(Fo=0) = 1, \quad \theta(X=0) = 0, \quad \theta(X=1) = 1 \tag{5}$$

$$\frac{\partial \theta}{\partial X}(X=\Delta) = \frac{1}{Ste}\frac{d\delta}{dFo}. \tag{6}$$

Imposing the energy balance at the phase boundary, the analytical solution of Eq. (4) yields the relation

$$\frac{\Delta\sqrt{\pi}}{2\sqrt{Fo}} \cdot exp^{\left(\frac{\Delta^2}{4Fo}\right)} \cdot erf\left(\frac{\Delta}{2\sqrt{Fo}}\right) = Ste. \tag{7}$$

More details of the analytical solution are given in Refs. [15–17]. The dimensionless solidification thickness (Δ) is thus a function of

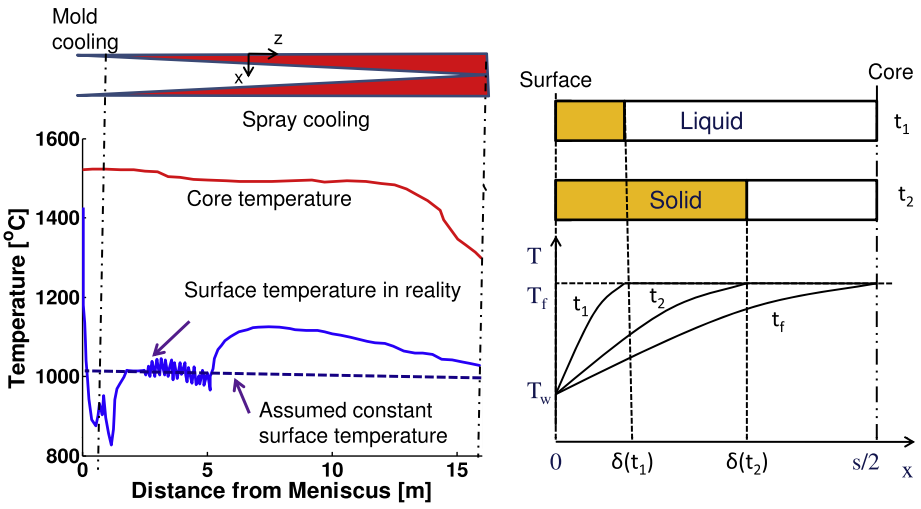

Fig. 1. Temperature profile of an ingot during the continuous casting process and theoretical model.

the Fourier number (Fo) and Stefan number (Ste). The above expression can be applied to the continuous casting process as follows: a) for a given cast material and constant surface temperature, Ste can be calculated. b) for a certain amount of solidification thickness, Fo can be calculated from Eq. 7. c) convert the Fo to solidification length. This procedure is valid for different alloys that can be cast continuously with an assumption of constant surface temperature. Now, for the complete solidification, $\Delta = 1$ and $Fo = Fo_f$. The relation between Fo_f and Ste can be modified as

$$\frac{1\sqrt{\pi}}{2\sqrt{Fo}}\cdot exp^{\left(\frac{1}{4Fo_f}\right)}\cdot erf\left(\frac{1}{2\sqrt{Fo_f}}\right) = Ste. \tag{8}$$

From the Fourier number Fo_f, the total solidification time can be found as

$$t_f = Fo_f\cdot\frac{(s/2)^2}{a}. \tag{9}$$

The total solidification length can be calculated using t_f and V_c

$$L_f = t_f\cdot V_c. \tag{10}$$

The casting speed can be calculated from the mass flow rate $\dot{M}$ as,

$$V_c = \frac{\dot{M}}{\rho Bs}. \tag{11}$$

Finally, the total solidification length can be expressed as

$$L_f = \frac{c\dot{M}}{4\lambda}\cdot\frac{Fo_f(Ste, B/s)}{B/s}. \tag{12}$$

The solidification length is proportional to the mass flow rate, the specific heat and inversely proportional to the thermal conductivity. However, the above expressions are only valid for infinite slabs with one dimension greater than the other. The following section explains the procedure for finding the solidification length of finite slabs.

2.3. Finite slab

The heat conduction is typically two dimensional for a finite slab and the differential equation that governs the heat transfer is expressed as [15].

$$\rho c\frac{\partial T}{\partial t} = \lambda\left(\frac{\partial^2 T}{\partial x^2}+\frac{\partial^2 T}{\partial y^2}\right), \tag{13}$$

with initial and boundary conditions

$$T(x,y,t=0) = T_f \quad T(x=B/2,y,t) = T_w \quad T(x,y=s/2,t) = T_w. \tag{14}$$

Non dimensionalizing the above equations with $X = \frac{x}{B/2}$ and $Y = \frac{y}{s/2}$, the heat transfer equation is modified into

$$\frac{\partial\theta}{\partial Fo} = \frac{\partial^2\theta}{\partial X^2}+\frac{s^2}{B^2}\frac{\partial^2\theta}{\partial Y^2}. \tag{15}$$

The theoretical solution of the above equation is complex. Therefore, numerical method is used. In the numerical solution, the solidification effect (latent heat release) is incorporated by increasing the specific heat as follows [18]:

$$c = \begin{cases} c & if\ \ T<T_s \text{ or } T>T_l \\ c+\Delta h\dfrac{\partial f_l}{\partial T} & if\ \ T_s\le T\le T_l \end{cases} \tag{16}$$

where f_l is the liquid fraction. Finally, the non dimensionalized equations with the solidification effect for both infinite slab (Eq. (17)) and finite slab (Eq. (18)) cases are expressed as

$$\left(1+\frac{1}{Ste}\frac{\partial f_l}{\partial\theta}\right)\frac{\partial\theta}{\partial Fo_f} = \frac{\partial^2\theta}{\partial X^2} \tag{17}$$

$$\left(1+\frac{1}{Ste}\frac{\partial f_l}{\partial\theta}\right)\frac{\partial\theta}{\partial Fo_f} = \frac{\partial^2\theta}{\partial X^2}+\frac{s^2}{B^2}\frac{\partial^2\theta}{\partial Y^2}. \tag{18}$$

3. Results

The numerical solution is carried out using COMSOL Multiphysics 4.3a. The accuracy of the numerical solution is checked for the semi infinite slab case. The boundary conditions in both regular and non dimensionalized forms are shown in Fig. 2. The analytical expression in Eq. (8) and the solution of Eq. (17) are plotted in Fig. 3. In the numerical solution, first *Ste* value is fixed and the governing equation is solved for Fo_f. Then, the *Ste* value is varied from 0.4 to 2 and in each case Fo_f is recorded. Fig. 3 shows that there is a good agreement between the analytical and numerical solutions. The method can be easily extended to low or high Stefan numbers if needed. However, a low *Ste* number can produce numerical challenges and the solution strongly depends on the fictitious phase change interval, mesh size and time step [18]. From Fig. 3, simple expressions can be formulated for finding the solidification of semi infinite slabs. For steel alloys, by approximating the function between Ste and Fo_f as linear (Fig. 3), the expression for L_f can be expressed as

$$L_f = \frac{c\dot{M}}{4\lambda}\cdot\frac{s}{B}\cdot\left(0.63 - 0.11\cdot c\cdot\frac{T_f - T_w}{\Delta h}\right). \quad (19)$$

Similarly for copper alloys, the linearized expression for L_f can be expressed as

$$L_f = \frac{c\dot{M}}{4\lambda}\cdot\frac{s}{B}\cdot\left(2.4 - 2.5\cdot c\cdot\frac{T_f - T_w}{\Delta h}\right). \quad (20)$$

From Fig. 3, it can be observed that the slope of the curve is more steeper for lower Ste than for the high Ste. This means that the change in surface temperature effects greatly the solidification time of copper than steel.

For finite slabs, first the geometric parameter B/s ratio and *Ste* are fixed and Eq. (18) is solved for Fo_f. Then the B/s ratio is fixed and *Ste* is varied from 0.4 to 2 and the corresponding Fo_f in each case is recorded. After this, the B/s ratio is changed from 1 to 2 in steps and similar trials are carried out. Fig. 4 shows the variation of Fo_f with *Ste* for various B/s ratio values. The B/s ratio equal to one represents the square cross section and more than one represents the rectangular cross sections. It can be observed that, the square cross section ($B/s = 1$) and 1-D infinite width plate ($B/s = \infty$) bounds the lower and upper limits in Fo_f vs *Ste* curve as shown in Fig. 4. At B/s ratio of nearly 1.8, the solution of the finite slab approximately equal to the infinite slab. It can be inferred that two dimensional

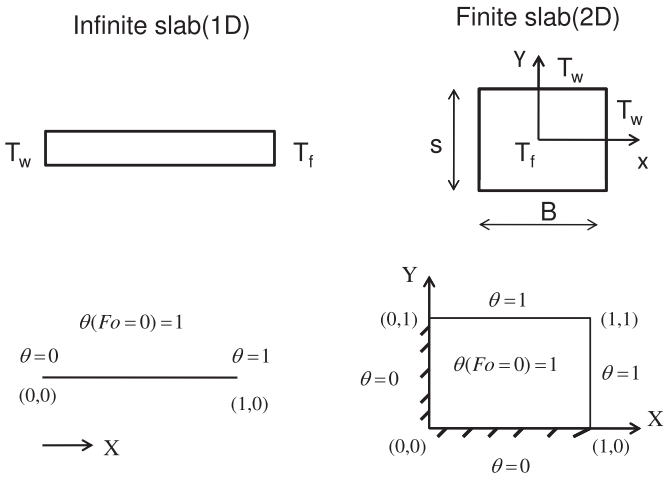

Fig. 2. Boundary conditions for the numerical problem for infinite and finite slabs.

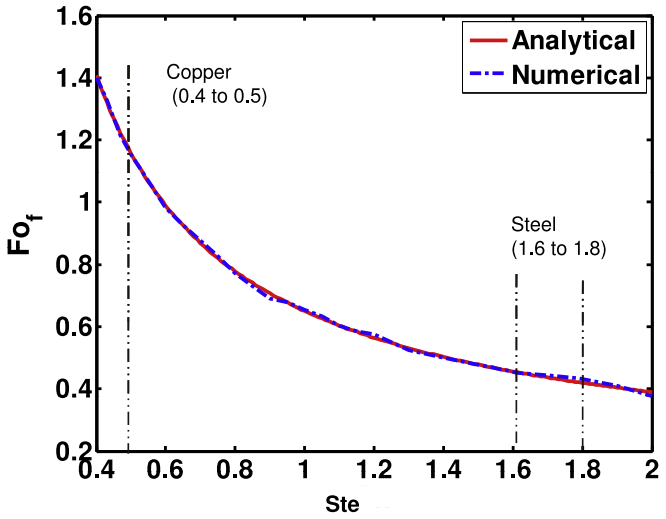

Fig. 3. Ste vs Fo_f for one dimensional slab.

cross sections with a width greater than 1.8 times the thickness can be considered as one-dimensional plate for the heat transfer analysis. This fact can be visualized further in Fig. 5. For the copper alloys, *Ste* falls in the range of 0.4–0.5 and the variation of Fo_f for various values of B/s ratio is plotted. Freezing Fourier number gradually increases with B/s ratio till 1.4 and stays constant for higher values of B/s. For the steel alloys, *Ste* is assigned as 1.75 and the variation of Fo_f for various B/s ratio values is plotted. The Fo_f gradually increases with the B/s ratio till 0.44 and stays constant for higher values of B/s. For fixed *Ste* values of 1.75 and 0.4, which are typical for the solidification of steel and copper alloys, the freezing Fourier number Fo_f for various B/s ratios can be calculated from Fig. 4. This Fo_f value can be used to find the solidification length (Eq. (12)).

Fig. 6 shows the effect of B/s ratio on the solidification length for various mass flow rates. The solidification length linearly increases with mass flow rate. The solidification length decreases with increase in B/s ratio except for small range of B/s ratio. A peak value is observed in the solidification length vs B/s plot (Fig. 6), which does not have any physical meaning. From Eq. (12), the first and second

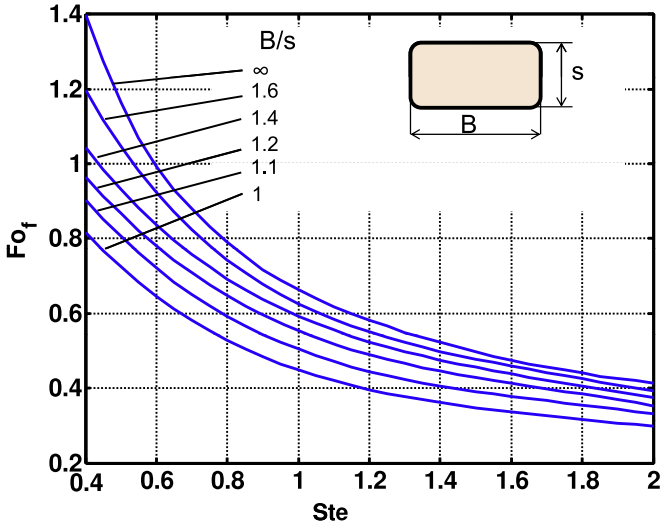

Fig. 4. Final Fourier number vs Stefan number for finite slabs.

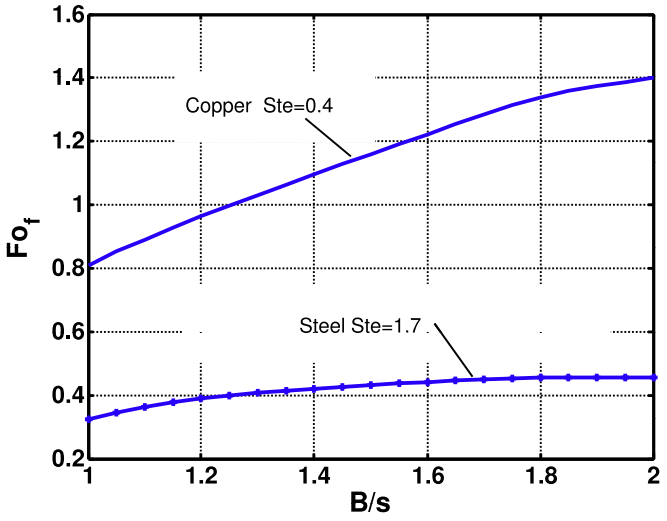

Fig. 5. Final Fourier number vs width to thickness ratio.

derivatives of the function L_f ($\frac{dL_f}{dB/s}$ and $\frac{d^2L_f}{d(B/s)^2}$) showed a maximum value for L_f at B/s = 1.09. Even though the peak value can be acceptable from the numerical perspective, the physical explanation for this peak is still a open question.

From the design point of view, it can be inferred that fixing the B/s ratio to as high as possible decreases the solidification length. But, too high of a B/s ratio is not suitable if the ingot is supposed to be sent through the rolling mills, which produces wire/coils. There should be a compromise between the solidification and rolling departments in fixing the B/s ratio. Similar trends are also observed for copper alloys. *Ste* is fixed as 0.4 and for various values of B/s ratio and various mass flow rates the solidification length is calculated. The effect of B/s ratio is almost negligible for copper alloys due to high thermal conductivity.

The solidification length for the copper casting presented in Fig. 6 may not match with the industrial results. The solidification of copper alloys is in general about 5–7 m. The copper alloys are generally cast using a twin-belt caster, where the caster length is about 3–4 m. The model discussed above neglects the variations of the surface temperature in the mold region and assumes a constant surface temperature from the start of solidification. For copper alloy casting in a twin-belt caster, the caster length cannot be neglected in comparison to the total solidification length.

The solidification length strongly depends on the cooling condition at the surface. To study this effect, the surface temperature is varied from850 °C to 1050 °C. It affects the *Ste* to change from 1.6 to 1.8 for steel. For a fixed B/s ratio, the freezing Fourier number Fo_f for various *Ste* can be calculated from Fig. 4. These Fo_f values are used to find the solidification length. Fig. 7 shows that the solidification length for all mass flow rates increases with surface temperature. A change in surface temperature of 50 °C changes the solidification length approximately to 1 m. Table 1 compares the theoretically estimated solidification length with the real time values for different industries. The deviation between theoretical and practical values is because of neglecting the temperature drop inside the mold in the theoretical solution.

Finally, the heat flux at the surface can also be derived. For a particular alloy with a fixed mass flow, the heat flux is inversely proportional to the square root of the distance from the meniscus. For a B/s ratio equal to one, and Fo_f value of 0.43, the heat flux is

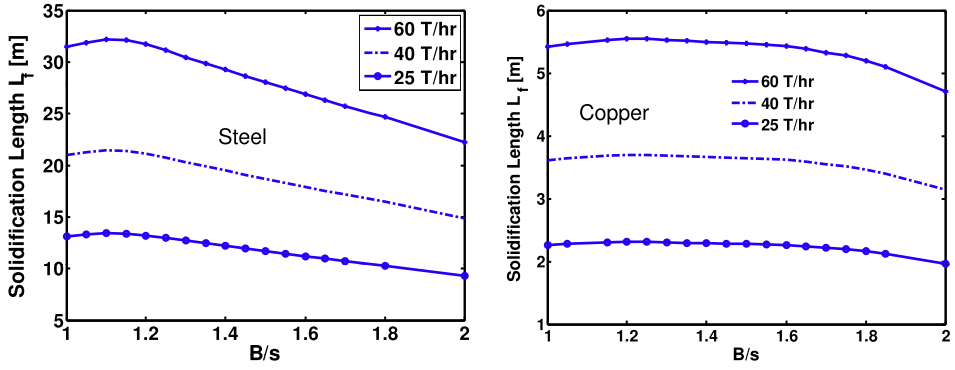

Fig. 6. Variation of solidification length with B/s ratio.

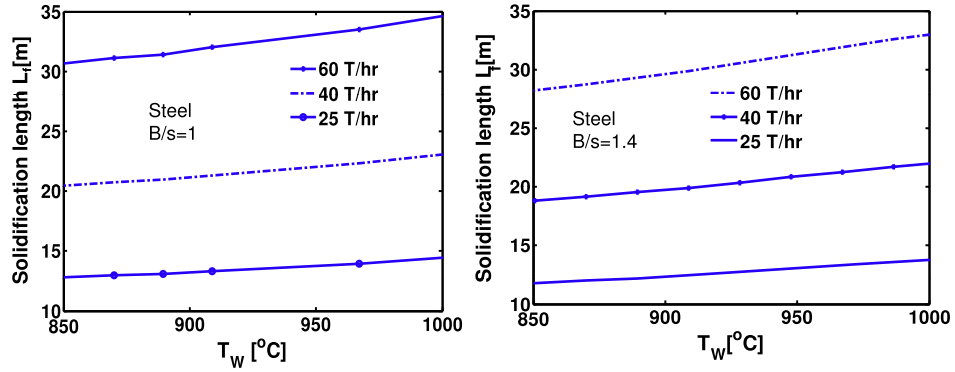

Fig. 7. Variation of solidification length with surface temperature.

Table 1
Comparison of theoretical and practical solidification length for different industrial casters.

Industry	B × s mm × mm	B/s	T_f °C	T_w °C	c J/kgK	λ W/mK	Δh kJ/kg	Ste	Fo_f	$\dot{M}$ t/h	L_f Theor	L_f Pract
SWISS STEEL [19]	150 × 150	1	1550	1000	700	30	272	1.68	0.42	22	15.1	15.2
UGITECH (Steel) [20]	205 × 205	1	1490	1100	700	30	207	1.32	0.38	21	12.8	13.8
THYSSEN KRUPP (Steel) [21]	1400 × 63	22.2	1550	1000	700	30	272	1.4	0.45	70	8.3	9.7
CONTIROD (Copper) [22]	120 × 70	1.7	1150	900	380	300	205	0.45	0.45	45	5.0	5.2

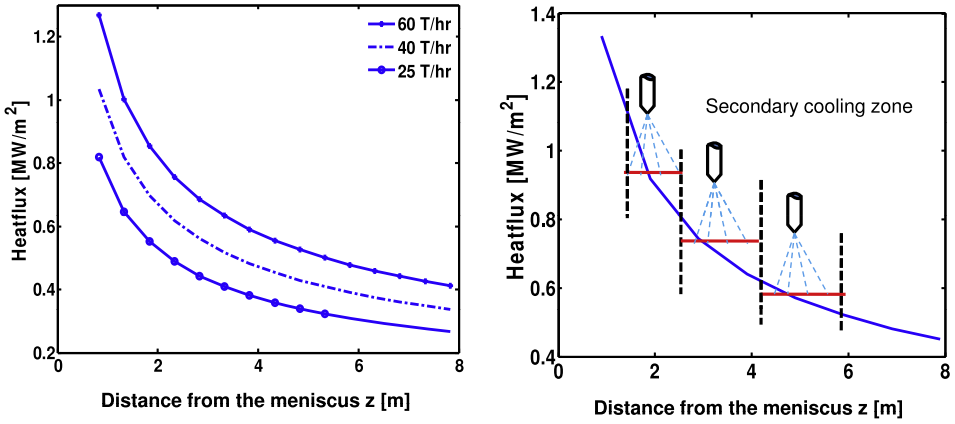

Fig. 8. Heat flux as a function of distance from the meniscus.

plotted in Fig. 8. The heat flux increases with the increase in mass flow rate. The plot provides the information about the heat flux to be applied in the secondary cooling zone to maintain the constant surface temperature. This heat flux can be achieved in reality by using the spray nozzles arranged at regular intervals in this zone.

4. Concluding remarks

Theoretical investigations are done to find the solidification length of continuous casting where the assumption of constant surface temperature is valid in the entire casting process. It can be summarized that,

1. Fourier and Stefan numbers, mass flow rate, specific heat, conductivity, and ingot geometry are the influencing parameters which governs the total solidification length.
2. The solidification length depends purely on the geometric ratio *B*/*s*, rather than the actual ingot dimensions (B and s).
3. The solidification length increases with mass flow rate and decreases with width to thickness ratio except for small values.
4. The change in the surface temperature affects greatly the solidification time of copper than the steel.
5. Steel requires a solidification length of nearly 6 to 7 times longer than copper.

Acknowledgments

The financial support provided by the German Science Foundation (DFG) through graduate school GRK1554 is sincerely acknowledged.

References

[1] J. Stefan, Über die Theorie der Eisbildung insbesondere über die Eisbildung im Polarmeere, Ann. Phys. Ges. 42 (1891) 269–286.
[2] J.K. Brimacombe, Empowerment with knowledge-toward the intelligent mold for the continuous casting of steel billets, Metall. Trans. B 24B (1993) 917–935.
[3] J.K. Brimacombe, P.K. Agarwal, S. Hibbins, B. Prabhakar, L.A. Baptista, in: J.K. Brimacombe, I.V. Samarasekera, J.E. Lait (Eds.), Continuous Casting, Heat Flow, Solidification and Crack Formation, vol. II, 1984, pp. 109–123.
[4] A. Grill, K. Sorimachi, J.K. Brimacombe, Heat flow, gap formation and breakouts in the continuous casting of steel slabs, Metall. Trans. B 7B (1976) 177–189.
[5] M. Alizadeh, A.J. Jahromi, O. Abouali, New analytical model for local heat flux density in the mold in continuous casting of steel, Comput. Mater. Sci. 44 (2008) 807–812.
[6] G. Straffelini, L. Lutterotti, M. Tonolli, M. Lestani, Modeling solidification microstructures of steel round billets obtained by continuous casting, ISIJ Int. 51 (2011) 1448–1453.
[7] Y.A. Meng, B.G. Thomas, Heat transfer and solidification model of continuous slab casting: CON1D, Metall Mater. Trans. B 34B (2003) 685–705.
[8] J.S. Ha, J.R. Cho, B.Y. Lee, M.Y. Ha, Numerical analysis of secondary cooling and bulging in the continuous casting of slabs, J. Mater. Process. Technol. 113 (2001) 257–261.
[9] B. Sarler, R. Vertnik, A.Z. Lorbiecka, I. Vusanovic, B. Sencic, A multiscale slice model for continuous casting of steel, IOP Conf. Series, Mater. Sci. Eng. 33 (2012) 012021.
[10] H. Wang, G. Li, Y. Lei, Y. Zhao, Q. Dai, J. Wang, Mathematical heat transfer model research for the improvement of continuous casting slab temperature, ISIJ Int. 45 (2005) 1291–1296.
[11] C.J. Petry, Hazelett twin belt caster, Light Metal. Age 15 (1975) 34–37.
[12] B. Farouk, D. Apelian, Y.G. Kim, A numerical and experimental study of the solidification rate in a twin-belt caster, Metall Mater. Trans. B 23B (1992) 477–492.
[13] A.G. Gerber, A.C.M. Sousa, A parametric study of the hazelett thin-slab casting process, J. Mater. Process. Technol. 49 (1995) 41–56.
[14] T.L. Bergman, A.S. Lavine, F.P. Incropera, D.P. Dewitt, Fundamentals of Heat and Mass Transfer, Wiley Publishing Inc, 2006.
[15] H.S. Carslaw, J.C. Jaeger, Conduction of Heat in Solids, Oxford University Press, 1959.
[16] E. Specht, Wärme-und Stoffübertragung in der Thermoprozesstechnik, Vulkan Verlag, 2014.
[17] P.K. Penumakala, Thermomechanical Simulation of Continuous and Semi-continuous Casting of Metals, Ph.D. thesis, Otto von Guericke University, Magdeburg, 2014.
[18] A.K. Nallathambi, E. Specht, A. Bertram, Computational aspects of temperature-based finite element technique for the phase change heat conduction problem, Comput. Mater. Sci. 47 (2) (2009) 332–341.
[19] Process Development, 2014. www.swiss-steel.com.
[20] C. Deville-Cavellin, A heat transfer model for UGITECH continuous casting machine, in: COMSOL Conference Hannover, 2008.
[21] Plant Layout, 1999. www.thyssenkrupp-steel.com.
[22] Hazelett Copper Bar Casting Machines, 2010. www.hazelett.com.